

HOBs methods for enhancing resolution and sensitivity in small DNA oligonucleotide NMR studies

Josiah M. McKenna^{†§} and John A. Parkinson^{†*}

[†]WestCHEM Department of Pure and Applied Chemistry, University of Strathclyde, 295 Cathedral Street, Glasgow, G1 1XL, U. K.

*Corresponding author:

Dr. John A. Parkinson
WestCHEM Department of Pure and Applied Chemistry¹
University of Strathclyde
295 Cathedral Street
Glasgow G1 1XL
United Kingdom

Email: john.parkinson@strath.ac.uk

Tel: +44 141 548 2820

Fax: +44 141 548 4822

[§]Visiting Thronson Scholar, Carroll University, 100 NE Ave, Waukesha, WI 53186, United States of America.

Abstract

^1H NMR spectra from biopolymers give chemical shifts classified according to proton type and often suffer from signal degeneracy. Data from nucleic acids are particularly prone to this failing. Recent developments in proton broad-band decoupling techniques with the promise of enhanced resolution at full sensitivity have allowed us to investigate the application of homo-nuclear band-selective (HOBS) decoupling to the study of small synthetic DNA molecules and to compare these with results from classical and Pure Shift techniques. Improved signal resolution at full sensitivity in both HOBS-1D ^1H and HOBS-2D [^1H , ^1H] NOESY NMR data are reported for three example small DNA molecules. Comparisons of ^1H T_1 and integrals of signals from HOBS-1D ^1H and HOBS-2D [^1H , ^1H] NOESY NMR data with those of standard data collection methods are also reported. The results show that homo-nuclear HOBS-NOESY data are useful for data assignment purposes and have some merit for quantification purposes. In general we show that resolution and sensitivity enhancement of ^1H NMR data for small DNA samples may be achieved without recourse to higher magnetic field strengths at full sensitivity in a band-selected manner.

Key Words: NMR, ^1H , DNA, band-selective homo-nuclear decoupling, HOBS, NOESY, T_1

Introduction

NMR studies of nucleic acids and their covalent and non-covalent complexes with ligands have provided rich information on the solution phase context of DNA and RNA as a complement to many studies carried out in the solid state by X-ray crystallography.^[1] The advantage of using small, synthetic DNA samples for solution phase NMR studies is the ready supply of sequence-defined molecules. A disadvantage, however, is that such material is mainly created without spin-isotope enrichment, which would typically ease the NMR data assignment process while adding richness to the information pool. Lack of isotope enrichment owes its absence on the one hand to high costs associated with producing synthetic, isotope-enriched DNA by solid-phase synthesis, or on the other in the specialized and somewhat involved process of isotope-enriched DNA production from cell-based growth methods.^[2-4] The limited palette of four nucleotides used as synthetic building blocks compared with twenty or so amino acid building blocks used for peptide and protein construction combines with often limited topological variation for DNA. The resulting DNA NMR spectra have very limited signal dispersion. By placing reliance largely on the use of ^1H NMR data to understand DNA solution behaviour in the absence of carbon or nitrogen spin-isotope enrichment, such poor signal dispersion, even at the highest available magnetic fields, can be limiting for the size and sequence length of even small DNA molecules that may be studied. This restricts the extent to which routine DNA solution phase NMR studies can be useful.

Any promise of improving signal resolution and dispersion is therefore attractive for potentially enhancing the applicability of NMR methods to the study of larger DNA molecules. Workable solutions for simplifying ^1H NMR spectra by eliminating evidence of scalar coupling (*i.e.* delivering spectra with a single resonance for each type of proton environment)^[5-8] depended initially on post data-acquisition processing tools to reconstruct NMR data suitable for handling *via* Fourier transform algorithms within commonly available software applications. These approaches proved that acceptable homo-nuclear broadband decoupled ($^1\text{H}\{-^1\text{H}\}_{\text{BB}}$) proton NMR data could be created and also showed great promise in the context of simplifying two-dimensional NMR data.^[9-11] However, the need for extended data acquisition periods and specialized post-acquisition processing macros meant that this type of approach to generating $^1\text{H}\{-^1\text{H}\}_{\text{BB}}$ NMR data was not ideal, particularly for non-

specialists within open-access NMR laboratories. Recently, a breakthrough in generating ^1H - $\{^1\text{H}\}_{\text{BB}}$ NMR data was reported with the creation of Pure Shift ^1H NMR data in real time using explicit data acquisition that incorporates repeated scalar coupling refocusing periods interleaved with data acquisition blocks.^[12] The approach brings ^1H - $\{^1\text{H}\}_{\text{BB}}$ NMR data acquisition into the main stream provided appropriate hardware capabilities are in place.

Although promising as a method for simplifying ^1H NMR data from biologically significant molecules including DNA, the technique suffers from a major drawback: the approach is very insensitive owing to spatial encoding which is required to generate ^1H - $\{^1\text{H}\}_{\text{BB}}$ NMR data. To overcome this issue, various modifications have been proposed. On the one hand, homo-nuclear band-selective decoupling (HOBS) allows data acquisition at full sensitivity but only on part of the NMR spectrum under special conditions.^[13,14] On the other hand, Pure Shift yielded by chirp excitation (PSYCHE) gives the full ^1H - $\{^1\text{H}\}_{\text{BB}}$ NMR spectrum reportedly with 10-fold greater sensitivity compared with the spatially encoded Pure Shift approach.^[15] HOBS is effective only if resonances from specific types of proton occur in a region of the spectrum that is relatively isolated from scalar coupling partners and allows full sensitivity to be maintained. This is a feature of particular interest when considering low concentrations of biopolymers. The success of the approach has been demonstrated for the peptide cyclosporine^[13] and is suitable for peptides and proteins in general. Conditions appropriate for using HOBS on peptides are similarly suitable for small, unlabelled DNA samples. In particular, the isolated aromatic region of the ^1H NMR spectrum of DNA contains cytosine H6 resonances, which may in theory be decoupled using the HOBS approach. Still greater benefit potentially arises by application of HOBS to the H1'/H5 resonance region of DNA ^1H NMR spectra. Only singlet resonances would be expected for all H1' and H5 resonances, potentially significantly enhancing signal resolution at full sensitivity without the need for increasing the magnetic field strength to achieve the same ends. In this report, we show how HOBS-style ^1H NMR data acquisition can be exploited to improve the resolution, sensitivity and overall quality of ^1H NMR data arising from small DNA samples and we compare some of these results with those arising from Pure Shift data acquisition. We demonstrate the benefit of using HOBS in the context of homo-nuclear correlation data when low millimolar concentrations of longer DNA sequences are studied and discuss some of the useful features that arise from acquiring such NMR data.

Experimental Section

Materials

The single stranded DNA sample d(GCCTGC) (6-mer) and self-complementary DNA duplex samples d(CGATATATCG)₂ (10-mer) and d(CGACGCGTACGCGTCG)₂ (16-mer) were manufactured on 15 μmol scale syntheses by AlphaDNA (Quebec, Canada) and were used without further purification. D₂O was purchased from Sigma-Aldrich and used as supplied.

Sample Preparation

DNA samples were freeze-dried once from D₂O solution and redissolved at the appropriate concentration in D₂O prior to being admitted to 5 mm Ø Wilmad 528-PP NMR tubes. The concentrations of the 6-mer, 10-mer and 16-mer samples were, respectively, 4.7 mM, 3.5 mM and 2.1 mM.

NMR data acquisition

All NMR data were acquired using a Bruker 14.1 T AVANCE II+ NMR spectrometer operating at 600.13 MHz for proton resonance using a triple resonance TBI [¹H, ¹³C, ³¹P-¹⁵N] probe-head fitted with an actively shielded z-gradient coil capable of delivering a maximum pulsed field-gradient field of 53.5 G/cm and running under Topspin (version 2.1, Bruker, Karlsruhe, Germany). All NMR data were acquired at a regulated probehead temperature of 298 K.

T₁ NMR data were acquired using standard and HOBS-adapted procedures as detailed later in the text: typically an 8 s relaxation delay period was followed by a 2 s solvent presaturation period after which the main pulse sequence ran. A variable delay (vd) list was used to generate data for the evaluation of T₁ parameters where vd = 100 μs, 0.1 s, 0.2 s, 0.5 s, 1 s, 2 s, 5 s, 10 s. T₁ values were estimated from triplicate data by fitting either peak intensities or integrals according to the standard expression $I_t = I_0 + P e^{-t/T_1}$. Data were compared between standard and HOBS-adapted pulse sequences for a selection of resonances for the model single-stranded oligonucleotide d(GCCTGC).

1D ¹H and 2D [¹H, ¹H] NOESY NMR data were acquired on the model single strand 6-mer d(GCCTGC) and on the 10-mer and 16-mer DNA duplexes. With the exception of the

spatially encoded Pure Shift data, solvent suppression was achieved by continuous low power irradiation of the residual $\underline{H}OD$ resonance typically at $\delta^1H = 4.709$ ppm. Typical 1D 1H NMR spectra were acquired with a 90° read pulse and with 16 - 64 transients over a 5.5 kHz frequency width centred at $\delta^1H = 4.709$ ppm. 1D- 1H -HOBS NMR spectra were acquired under similar conditions but additionally used a selective single pulsed-field gradient spin-echo employing a reburp shaped pulse calibrated for selective refocusing over bandwidths of between 0.6 and 1.2 kHz. 1D 1H instantaneous Pure Shift (HOBB) $^1H\{-^1H\}_{BB}$ NMR data were acquired with 8192 transients over a frequency width of 6 kHz. 2D standard NOESY, zero-quantum suppressed NOESY and their band-selective non-HOBS and HOBS equivalents were all acquired with presaturation using low-powered continuous irradiation at the transmitter offset frequency. All data were processed within Topspin 2.1.

Results and Discussion

Comparison of standard, broadband homo-decoupled (HOBB) and band-selected homo-decoupled (HOBS) data.

The assumption that specific regions of 1H NMR spectra from oligonucleotides would benefit from increased resolution and signal intensity arising from HOBS-style NMR data acquisition compared with standard NMR data acquisition was tested with the model 6-mer oligonucleotide d(GCCTGC). This exists predominantly in single strand form under the sample conditions used.^[16] Standard 1D 1H NMR data acquired with solvent presaturation using a 90° read pulse were typical of similar data found for short oligonucleotides reported in the literature and showed classical effects from J -couplings (**Figure 1a, d and g**). Comparison with data from broadband homo-nuclear decoupling (Pure Shift/HOBB data acquisition, **Figure 1b, e and h**) using an instantaneous, on-the-fly chunking approach^[12] revealed the instant resolution benefit that was predicted to occur through such data acquisition schemes. In the aromatic resonance region, the doublet resonances for C^3H6 , C^2H6 and C^5H6 ($\delta^1H = 7.939, 7.669$ and 7.637 ppm respectively, **Figure 1a**) collapsed to singlets as expected (**Figure 1b**). Simplification of the data was similarly apparent across the spectrum and in particular in the $H1'/H5$ resonance region $\delta^1H = 6.4$ - 5.4 ppm as predicted. Here, all J -coupling information was eliminated and each signal appeared as a pure singlet (**Figure 1e**). Simplification of the $H2'/H2''$ resonance region ($\delta^1H = 3.0$ - 2.0 ppm) was also

apparent, although as expected some coupling information was retained owing to the close chemical shift of H2'/H2'' partner resonances (**Figure 1h**). Although these results appear excellent, the acquisition time required to attain quality HOBB (Pure Shift) data was excessive for a 1D ^1H NMR spectrum (9 hours 37 minutes). Nevertheless, the data proved the principle that even low millimolar concentrations of small DNA oligonucleotides can be analysed by ^1H NMR using such a Pure Shift approach. In contrast, as shown by **Figure 1c, f** and **i**, the issue of sensitivity with simplification of data can be readily addressed using the HOBS approach for oligonucleotides. These HOBS data were each acquired at full sensitivity in just over a minute rather than several hours taken to acquire the Pure Shift (HOBB) data. They also demonstrated how, by the use of a band-selective approach with on-the-fly data chunking, the oligonucleotide 1D ^1H NMR spectral resolution and sensitivity can be significantly improved in specific regions of DNA NMR spectra. For the aromatic and H1'/H5 resonance regions in particular, all observed signals collapsed to reveal only resolved singlets at each chemical shift (**Figure 1c** and **f**). Although some couplings were inevitably retained in the H2'/H2'' resonance region (**Figure 1i**) compared with the equivalent Pure Shift data (**Figure 1h**) the improvement in signal resolution for the HOBS data is nevertheless impressive.

Figure 1: Aromatic (**a-c**), H1'/H5 (**d-f**) and H2'/H2''/CH₃ (**g-i**) resonance regions of 600 MHz 1D ^1H NMR data for the 6-mer oligonucleotide d(GCCTGC) in D₂O at a concentration of 4.7 mM acquired using a variety of acquisition modes. **a), d), g):** 1D ^1H NMR spectrum acquired using a standard single-pulse/acquire scheme with presaturation using 16 transients; **b), e), h):** 1D ^1H NMR spectrum acquired using an instantaneous Pure Shift (HOBB) acquisition scheme with presaturation using 8192 transients; **c), f), i):** 1D ^1H NMR spectrum acquired with 16 transients using a band-selected homo-decoupling (HOBS) acquisition scheme in which each spectrum was acquired under separate acquisition conditions using frequency shifted band-selective reburp pulses: **c)** – bandwidth = 550 Hz, selective pulse offset frequency = 1670.2 Hz; **f)** – bandwidth = 600 Hz, selective pulse offset frequency = 710.5 Hz; **i)** – bandwidth = 1200 Hz, selective pulse offset frequency = -1713.73 Hz. Note that the sample used has been aged in D₂O resulting in the guanine H8 resonances exchanging over time with deuterium. Hence these resonances are not observed in the data (see **Figure S1** in the Supporting Information).

The improvement in resolution noted for the 6-mer single strand d(GCCTGC) was also found in the more realistic contexts of the 10-mer and 16-mer self-complementary DNA duplex molecules, which possess a greater number of base-pairs, furanose sugars and consequently H1', H5 and H6 resonances. The results (**Figure 2**) show marked improvement in resolution as anticipated for the HOBS-style data compared with the fully-coupled data acquired under single pulse/acquire conditions. Both aromatic and H1'/H5 resonance regions are substantially better resolved at no cost in signal-to-noise, making it clear that the HOBS-style technique is highly applicable to the study of longer DNA molecules in solution owing to the improved spectral resolution with no change in magnetic field strength.

Figure 2: 600 MHz 1D ^1H NMR spectra of DNA duplexes acquired with and without HOBS-style data acquisition. **a)** 10-mer duplex d(CGATATATCG)₂ standard data acquisition; **b)** as for **(a)** but with HOBS-style data acquisition; **c)** 16-mer duplex d(CGACGCGTACGCGTTCG)₂ standard data acquisition; **d)** as for **(c)** but with HOBS-style data acquisition. Spectra **(b)** and **(d)** showing HOBS data are each a combination of HOBS spectra acquired over different frequency-selected regions followed by co-addition of the spectra post-processing. All contributing spectra were acquired with 16 transients per FID over a frequency width of 5.5 kHz.

To check the integrity of the HOBS NMR data by comparison with data arising from a standard acquisition scheme, we integrated those resonances that were clearly resolved in each case and compared the results. We also compared integrals from clusters of resonances that remained unresolved in the standard 1D ^1H NMR spectrum of d(GCCTGC). The results shown in **Table 1** suggest that in large part, integrals from the HOBS- ^1H NMR data and those from the standard 1D ^1H NMR data are comparable, meaning that the HOBS data may, with care, be used to determine the numbers of protons of particular types by integration. Whilst this is rudimentary for small molecules of the type used to generate these data, it is unlikely that integration in one dimension would be used for larger oligonucleotides, due to signal overlap even in HOBS-type data. Nevertheless the principle of reliable integration is important to establish for such data acquisition styles, especially if this is considered in relation to the integration of 2D NOESY NMR data for the purposes of

extracting information about inter-proton distances when used in solution phase structure determination studies as detailed later in this article.

With this in mind, we also investigated how results from T_1 NMR relaxation data measurements might be affected through HOBS-style data acquisition as a prelude to evaluating the feasibility of using 2D HOBS- ^1H NOESY NMR data for inter-proton distance determination for DNA molecules. Our suspicions regarding this were aroused when we assessed the effects of altering the relaxation delay for the HOBS-style data acquisition compared with a single-pulse/acquire data acquisition scheme. It was clear (Supporting Information **Figure S2**) that at the longer relaxation delays tested (d_1 values up to and including 5 s) with HOBS, the data were of greater intensity compared with those acquired with short relaxation delays (e.g. $d_1 = 1$ s). In contrast, data from a single-pulse/acquire scheme using the same range of relaxation delays showed very similar intensities to one another. A common practice in 2D [^1H , ^1H] correlation data acquisition schemes, especially for biopolymer samples, is to cut the relaxation delay back in order to shorten the overall time taken to acquire a complete data set, which is valid owing to the extent of the spin-relaxation networks in such biopolymers. For DNA samples, some resonances such as those arising from adenine H2 protons take longer to recover and longer relaxation times are therefore recommended when acquiring NOESY data for quantification. Results from the HOBS data acquisition scheme suggest that longer relaxation delays may be required as a matter of course with the benefit of creating data with greater signal intensity. As usual, the trade-off in time *versus* signal intensity should be considered carefully but it is apparent from these measurements that some care should be taken over the choice of relaxation delay when acquiring HOBS ^1H NMR data from small DNA oligonucleotide samples.

To explore this matter further, we evaluated T_1 relaxation parameters on the model 6-mer oligonucleotide using two schemes, one being a simple modification of the classical T_1 inversion-recovery experiment that incorporated instantaneous HOBS-style data acquisition (Supporting Information **Figure S3**) as reported in the recent work of Parella,^[17] in our case incorporating the trivial modification of presaturation to suppress the residual solvent signal. This allowed us to measure for the first time T_1 relaxation parameters with and

without band-selective homo-nuclear decoupling from small DNA oligonucleotide ^1H NMR spectra. Comparisons of these data were made as summarized in **Table 2**.

The data revealed good agreement between measurements made using standard inversion-recovery and HOBS inversion recovery to determine proton T_1 relaxation values in small DNA oligonucleotides, in accordance with conclusions drawn from the work on the peptide cyclosporine A in d_6 -benzene.^[17] The increased standard error in HOBS- T_1 data for C^3H_6 , $\text{C}^6\text{H}1'$, C^3H_5 , $\text{T}^4\text{H}1'$ and C^2H_5 is a reflection of the differences encountered through fitting data derived from peak intensity compared with peak area. Generally, those data that were only available for peak-picking from the standard T_1 inversion recovery approach (owing to signal overlap in J -coupled spectra) coincided more closely with those values derived from peak-integrated HOBS T_1 inversion recovery data for measurements made in triplicate (see Supporting Information **Tables S1-S4**). For example, the peak-picked, HOBS- T_1 data for $\text{C}^6\text{H}1'$ gave an average T_1 value over triplicate measurements equal to 1.669 ± 0.004 s. This deviated from the value obtained by integration of the same data which gave an average T_1 value of 1.848 ± 0.004 s. This more closely reflected the value obtained by peak-picking the same resonance using the standard T_1 inversion recovery data, which gave $T_1=1.831 \pm 0.016$ s. The other highlighted resonances with larger standard errors showed similar trends. This suggests that in our hands when studying small DNA oligonucleotides, peak intensity is a less reliable source for T_1 data fitting in a HOBS- T_1 style data acquisition mode compared with using peak integration on the same data. For this reason it is suggested that T_1 data fitting made using a HOBS-type instantaneous acquisition protocol is compared for results using both peak areas and peak intensities wherever possible to prevent misinterpretation. One explanation for the difference observed may be associated with the additional influence of T_2 relaxation on the FID that is created using the instantaneous acquisition protocol used in this work, which is a source of line-broadening effects.^[18]

Comparison of 2D [^1H , ^1H] HOBS-NOESY with standard and band-selected 2D [^1H , ^1H] NOESY.

The evidence shown by the improvement in spectral resolution achieved for longer DNA sequences using 1D ^1H HOBS suggested that similar benefit could also be achieved for 2D [^1H , ^1H] correlation data through relatively straight-forward modification of available pulse

sequences. We were particularly interested in exploring the extent to which 2D [^1H , ^1H] NOESY NMR data of DNA samples might be enhanced using HOBS following a recent report illustrating the application of NOESY adapted for HOBS in the context of peptide studies.^[18] Our approach began with basic pulse sequences to ensure that data acquisition worked, subsequently progressing to more advanced pulses sequences. Initially to test how HOBS might influence the generation of NOESY NMR data from small DNA oligonucleotides, three pulse sequences and their variants were created. These included those shown schematically in **Figure 3** alongside a classical 2D NOESY pulse sequence from which they were derived. A zero-quantum suppression NOESY pulse sequence (**Figure S4** in the Supporting Information) was also adapted and tested successfully as part of this process.

Figure 3: Pulse sequences from among those used to measure 2D [^1H , ^1H] NOESY NMR spectra for 6-mer, 10-mer and 16-mer oligonucleotides in D_2O . **a)** Basic pulse sequence used for the acquisition of band-selected NOESY NMR data without broadband homonuclear decoupling: $\phi_1 = x, -x$; $\phi_2 = x [8], -x [8]$; $\phi_3 = x, x, -x, -x, y, y, -y, -y$; $\phi_4 = -x, x, -x, x, y, -y, y, -y$; $\phi_{\text{rec}} = x, -x, -x, x, y, -y, -y, y, -x, x, x, -x, -y, y, y, -y$; $G_1 = 60\%$ with a 1 ms duration; **b)** Basic pulse sequence used for the acquisition of HOBS-style 2D [^1H , ^1H] NOESY NMR data: $\phi_1 = x, -x$; $\phi_2 = x [8], -x [8]$; $\phi_3 = x, x, -x, -x, y, y, -y, -y$; $\phi_4 = x, -x, -x, x, y, -y, -y, y$; $\phi_{\text{rec}} = x, -x, -x, x, y, -y, -y, y, -x, x, x, -x, -y, y, y, -y$; $G_1 = 60\%$, $G_2 = 23\%$ and $G_3 = 41\%$ with a 1 ms duration (δ). Sine-shaped gradient pulses were used throughout. Narrow black bars correspond to hard 90° pulses, wide black bars correspond to 180° pulses and soft 180° pulses are as indicated. A band-selective reburp pulse was used for selective inversion of magnetization.

The non-HOBS, band-selected NOESY pulse sequence (**Figure 3a**) allowed direct comparison to be made with data acquired using the HOBS-NOESY pulse sequence (**Figure 3b**), the former resulting in region-selected data in the presence of J -couplings while the latter resulted in region-selected data in the absence of J -couplings. These data were compared with those from a classical 2D NOESY acquisition scheme. Spectra were acquired for the 16-mer DNA duplex to demonstrate the feasibility of generating usable data sets. As shown (**Figure 4**) NOESY data for the non-HOBS and HOBS band-selected acquisition schemes (**Figures 4b** and **4c** respectively) faithfully reproduced the region from the full NOESY data

set (**Figure 4a**). The example shown selected the H1'/H5 resonance region of the spectrum to illustrate the effectiveness of the HOBS-style data acquisition for improving resolution in the ω_2 frequency domain. The region provides information on through-space interactions between H1'/H5 protons and H8/H6, H3', H4', H5'/H5'', H2'/H2'' and CH₃ protons. This substantial set of NOE information is sufficient to enable resonance assignments to be defined for a large number of protons in small DNA molecules. When combined with information arising from similar data acquired using a H8/H6 band-selective pulse, a complete set of ¹H resonance assignments for such a molecule is feasible. Similar data for the 10-mer DNA duplex d(CGATATATCG)₂ illustrating this fact are shown in the Supporting Information (**Figures S5** and **S6**). As shown by **Figure 4c** for the 16-mer, substantial improvement in resolution is achieved across the selected region using HOBS. There is no gain in time-saving using this approach and in practice, the non-HOBS and HOBS band-selected NOESY data sets were acquired with 16 transients per FID (**Figure 4b** and **4c**) into 8192 data points compared with the full data set for which 8 transients were acquired into 2048 data points per FID (**Figure 4a**) and in order to achieve the same ω_1 resolution, the same number of t_1 increments (360) were used to acquire all three data sets with all data being processed in the same manner.

Figure 4: 600 MHz 2D NOESY NMR spectra acquired for 2.1 mM d(CGACGCGTACGCGTCG)₂ in D₂O at 298 K. **a)** Standard NOESY data acquisition scheme; **b)** band-selected, *J*-coupled (non-HOBS) data acquisition scheme; **c)** band-selected homo-nuclear decoupled (HOBS) data acquisition scheme. Complete data sets are shown for **(b)** and **(c)** whereas **(a)** shows the equivalent region taken from a complete 2D-NOESY data set for the 16-mer. 1D ¹H NMR spectra are shown as projections appropriate to the 2D acquisition scheme used in each case.

The improvement in resolution in the HOBS-NOESY data compared with the band-selected and standard 2D-NOESY data sets is particularly well illustrated in the H1'/H5 to H4'/H5'/H5'' cross-peak region of the data acquired for the 16-mer DNA duplex (**Figure 5**) along with slices taken through the data (**Figure 6**). As these illustrations show, the advantage gained in resolution by using HOBS to acquire NOESY data for DNA is significant and could be used instead of a complete NOESY data set to define signal assignments more

clearly. The 16-mer DNA duplex, which possesses a repeat sequence of –ACGCGT–, has many degenerate ^1H NMR resonances, which belies the apparent simplicity of the data. Standard 2D [^1H , ^1H] NOESY NMR data cannot resolve many of the resonances but HOBS-type data shows promise in resolving normally overlapped resonances, thereby enabling a more rigorous signal assignment of the data.

Figure 5: Expansions showing the H1'/H5 to H4'/H5'/H5'' cross-peak region of the 600 MHz 2D NOESY NMR spectra acquired for d(CGACGCGTACGCGTCG)₂ in D₂O at 298 K. **a)** Standard NOESY data; **b)** band-selective, *J*-coupled (non-HOBS) data; **c)** band-selective homo-nuclear decoupled (HOBS) data.

Figure 6: Slices extracted at $\delta^1\text{H}(\omega_1) = 4.14$ ppm from each of the 2D [^1H , ^1H] NOESY NMR data sets for the 16-mer DNA duplex d(CGACGCGTACGCGTCG)₂ in D₂O. **a)** Standard NOESY data; **b)** band-selected, *J*-coupled (non-HOBS) NOESY data; **c)** HOBS-NOESY data. Note the improvement in signal resolution for the two resonances highlighted in the boxed region of the spectra, which show coincidence in **(a)** and **(b)** but are clearly resolved in **(c)**.

Use of HOBS-NOESY NMR data for inter-proton distance measurements

The question remaining is whether such data can be useful in the context of inter-proton distance measurements. In general and with a number of assumptions, NOESY cross-peak integrals are used to generate inter-proton distance values that may subsequently be used as restraints in molecular mechanics/dynamics calculations for determining solution-state structures of biomolecules. The NOE associated with two protons between which the accurate distance is known based on crystallographic evidence is used as a calibration value against which unknown distances may be determined from assigned NOEs. This process has always been compromised by overlapping cross-peaks. Increased resolution in theory would allow more accurate distances to be determined for more pairs of protons within a given molecule. Using the acquired NOESY data, we made a cursory study of whether HOBS-type NOESY data could be reliably used to extract such distance information alongside their use in determining signal assignments. To this end, we integrated the same set of specific cross-peaks in standard NOESY, band-selected NOESY and HOBS-NOESY data for the 16-mer DNA duplex d(CGACGCGTACGCGTCG)₂ and compared the values as normalized to a specific H6-

H5 NOESY cross-peak, labelled A (**Figure S7**), in each of the data sets. A visual representation of the location of each of the cross-peaks used is shown (**Figure S7** in the Supporting Information). **Table 3** summarizes the results of our findings.

To some extent, the integral values determined for the representative NOESY cross-peaks compare favourably between standard NOESY, band-selected NOESY and HOBS-NOESY (cross-peaks A-D, M-O, Q-V). However, some values show a marked (> 3 times) difference between those measured in standard NOESY data sets and those measured in either band-selected or HOBS-NOESY data sets (cross-peaks K, L, P, W) although the similarity in each case between integrals from band-selected and HOBS-NOESY is generally notable. All data were acquired and treated in the same manner and whilst good reproducibility is in evidence, it's clear that further rigorous investigations are required to confirm whether the differences observed are likely to be commonplace between data from standard NOESY compared with either band-selected- or HOBS-NOESY spectra before a clear judgement can be made concerning the use of HOBS-NOESY NMR data for quantitation relating to inter-proton distance evaluation for DNA samples. Overall the results are promising when combined with the effects of improved resolution.

Conclusions

In this work we have demonstrated for the first time the use of HOBS-type NMR data acquisition schemes for the simplification and resolution enhancement of ^1H NMR spectra from small DNA oligonucleotides by elimination of J -coupling through region selective broad-band homonuclear decoupling at full sensitivity. Our findings show that for these molecules, the result of using HOBS acquisition schemes do not affect the reproducibility of T_1 relaxation data compared with standard inversion recovery schemes used for T_1 measurements, in keeping with recent findings.^[17] We found that care should be taken to ensure that the relaxation delay is lengthened compared with classical schemes for 1D ^1H NMR data acquisition to allow full signal intensity to be achieved. Simplification of H1'/H5 and aromatic regions of DNA ^1H NMR spectra at full sensitivity is of real benefit in cases of longer DNA sequences that give more complex, overlapped NMR spectra. Application of the HOBS techniques in the context of 2D [^1H , ^1H] NOESY NMR data acquisition shows no loss in data integrity, indicating that such data may be acquired for signal assignment at higher

resolution than could normally be expected using standard acquisition schemes. Although similarities exist in the quantitation of NOESY cross-peaks from either band-selected- or HOBS-NOESY NMR data compared with standard NOESY NMR data for the same molecule, further detailed evaluation should be carried out using a range of acquisition conditions and different DNA samples before a clear judgement may be made on this. Nevertheless, our findings show that HOBS-NOESY NMR data for small DNA oligonucleotide samples may be used routinely to improve resolution for at least one half of the spectral width associated with DNA ^1H NMR spectra. Further work is in progress to explore the application of related techniques that may further enhance the quality and utility of such data.

Acknowledgements

JMM gratefully acknowledges Carroll University, Waukesha, USA, for the award of a Thronson Scholarship and the opportunity to complete his undergraduate research at the University of Strathclyde, U. K. We also thank Prof. Klaus Zangger, University of Graz, Austria for the initial discussion and dialogue over instantaneous Pure Shift methods and the provision of pulse sequence code adapted for instantaneous Pure Shift data acquisition.

References

- [1] For example see a) H. Y. Alniss, N. G. Anthony, A. I. Khalaf, S. P. MacKay, C. J. Suckling, R. D. Waigh, N. J. Wheate, J. A. Parkinson. *Chem. Sci.* **2012**, 3(3), 711-722. b) J. A. Parkinson, A. I. Khalaf, N. G. Anthony, S. P. Mackay, C. J. Suckling, R. D. Waigh. *Helv. Chim. Acta* **2009**, 92, 795-822. c) N. B. Ulyanov, W. R. Bauer, T. L. James. *J. Biomol. NMR* **2002**, 23(3), 265-280. M. Katahira, M. Kanagawa, H. Sato, S. Uesugi, S. Fujii, T. Maeda. *Nucl. Acids Res.* **1994**, 22(14), 2752-2759.
- [2] J. M. Louis, R. G. Martin, G. M. Clore, A. M. Gronenborn. *J. Biol. Chem.* **1998**, 273(4), 2374-2378.
- [3] J. Yan, J. H. Bushweller. *Biochem. Biophys. Res. Commun.* **2001**, 284, 295-300.
- [4] B. René, G. Masliah, L. Zargarian, O. Mauffret, S. Femandjian. *J. Biomol. NMR* **2006**, 36, 137-146.
- [5] K. Zangger, H. Sterk. *J. Magn. Reson.* **1997**, 124, 486-489.
- [6] A. J. Pell, R. A. E. Edden, J. Keeler. *Magn. Reson. Chem.* **2007**, 45, 296-316.
- [7] J. A. Aguilar, M. Nilsson, G. A. Morris, S. Faulkner. *Angew. Chem. Int. Ed. Engl.* **2010**, 49, 3901-3903.
- [8] N. H. Meyer, K. Zangger. *ChemPhysChem* **2014**, 15, 49-55.
- [9] G. A. Morris, J. A. Aguilar, R. Evans, S. Haiber, M. Nilsson. *J. Am. Chem. Soc.* **2010**, 132(37), 12770-12772.
- [10] J. A. Aguilar, A. A. Colbourne, J. Cassani, M. Nilsson, G. A. Morris. *Angew. Chem. Int. Ed. Engl.* **2012**, 51(26), 6460-6463.
- [11] M. Nilsson, G. A. Morris. *Chem. Commun.* **2007**, 933-935.
- [12] N. H. Meyer, K. Zangger. *Angew. Chem.* **2013**, 52(28), 7143-7134.
- [13] L. Castañar, P. Nolis, A. Virgili, T. Parella. *Chem. Eur. J.* **2013**, 19, 17283-17286.
- [14] V. M. R. Kakita, J. Bharatam. *Magn. Reson. Chem.* **2014**, 52, 389-394.
- [15] M. Foroozandeh, R. W. Adams, N. J. Meharry, D. Jeannerat, M. Nilsson, G. A. Morris. *Angew. Chem. Int. Ed. Engl.* **2014**, 53(27), 6990-6992.
- [16] M. P. Evstigneev, J. A. Parkinson, A. O. Lantushenko, V. V. Kostjukov, V. I. Pahomov. *Biopolymers* **2010**, 93(12), 1023-1038.
- [17] L. Castañar, P. Nolis, A. Virgili, T. Parella. *J. Magn. Reson.* **2014**, 244, 30-35.
- [18] J. Ying, J. Roche, A. Bax. *J. Magn. Reson.* **2014**, 241, 97-102.

Tables

Table 1: Comparison of integrals for individually resolved resonances and clusters of resonance for standard 1D ¹H and 1D ¹H-HOBS NMR data for selected regions.

Resonance (ppm)	Integral		Resonance (ppm)	Integral	
	1D ¹ H	1D- ¹ H HOBS		1D ¹ H	1D- ¹ H HOBS ^a
T ⁴ H6 (7.52) ^b	1.00	1.00	T ⁴ H1' (5.82) ^c	1.00	1.00
C ⁶ H6 (7.63)	1.02	0.93	G ⁵ H1' (6.17)	1.28	1.20
C ² H6 (7.67)	1.09	1.02	(6.33-6.24)	3.07	3.35 (0.85, 1.05, 1.45)
C ³ H6 (7.94)	0.90	0.66	(6.1-6.03)	1.87	1.98 (1.05, 0.93)
			(5.72-5.65)	1.49	1.69 (0.90, 0.79)

^aValues in brackets refer to integrals of individually resolved resonances in the HOBS data.

^bValue used as internal calibration reference for the remaining aromatic resonance integrals. ^cValue used as internal calibration reference for the remaining H1' and H5 resonance integrals.

Table 2: Comparison of ^1H T_1 relaxation time data for the oligonucleotide d(GCCTGC) in D_2O using standard T_1 inversion-recovery vs HOBS inversion-recovery according to the sequence shown in Supporting Information **Figure S3**.

$\delta^1\text{H}$ (ppm)	Assignment	T_1 (s) ^a	
		Standard-t1ir ^b	HOBS-t1ir
7.940	$\text{C}^3\text{H6}$	1.59 ± 0.01	1.50 ± 0.20
7.670	$\text{C}^2\text{H6}$	1.387 ± 0.001	1.39 ± 0.01
7.630	$\text{C}^6\text{H6}$	1.613 ± 0.002	1.61 ± 0.03
7.520	$\text{T}^4\text{H6}$	1.58 ± 0.02	1.61 ± 0.04
6.308	$\text{C}^6\text{H1}'$	1.83 ± 0.02	1.80 ± 0.10
6.292	$\text{C}^3\text{H1}'$	2.06 ± 0.01	2.11 ± 0.08
6.261	$\text{C}^2\text{H1}'$	1.70 ± 0.02	1.73 ± 0.03
6.173	$\text{G}^5\text{H1}'$	1.85 ± 0.02	1.89 ± 0.04
6.075	$\text{G}^1\text{H1}'$	1.89 ± 0.03	1.89 ± 0.04
6.057	$\text{C}^3\text{H5}$	2.50 ± 0.04	2.50 ± 0.10
5.816	$\text{T}^4\text{H1}'$	2.03 ± 0.03	2.00 ± 0.20
5.691	$\text{C}^6\text{H5}$	2.82 ± 0.05	2.84 ± 0.03
5.675	$\text{C}^2\text{H5}$	2.76 ± 0.04	2.90 ± 0.20

^aData are taken where possible as an average of T_1 determined by signal integration and by peak picking from data sets acquired in triplicate in each case. Further details are provided in Supporting Information **Tables S1-S4**. ^bt1ir – T_1 inversion recovery experiment.

Table 3: Comparison of normalized integrals for selected cross-peaks in different 2D [^1H , ^1H] NOESY NMR data sets acquired for the 16-mer DNA duplex d(CGACGCGTACGCGTCG)₂ in D₂O at 298K.

Peak ^a	¹ H Chemical Shift		Normalized Integral ^b		
	(ppm)		NOESY	NOESY-sel	NOESY-HOBS
	ω_1	ω_2			
A	7.542	5.823	1.000	1.000	1.000
B	7.414	5.616	0.650	0.686	0.622
C	7.169	5.177	1.131	1.121	1.503
D	7.107	5.114	0.937	0.950	1.272
K	4.023	4.846	0.717	0.234	0.255
L	4.253	4.846	0.854	0.303	0.274
M	3.989	4.894	0.310	0.204	0.294
N	4.219	4.890	0.152	0.081	0.098
O	4.068	5.547	0.446	0.391	0.554
P	2.501	4.846	0.636	0.201	0.163
Q	2.617	4.850	0.265	0.104	0.103
R	2.295	5.549	1.003	0.972	1.445
S	2.295	5.618	0.390	0.471	0.496
T	2.286	5.652	0.377	0.460	0.558
U	2.617	5.752	0.354	0.246	0.377
V	2.295	6.076	0.590	0.616	0.622
W	2.541	6.076	0.101	0.097	0.032

^aFor peak designation see **Figure S7** In the Supporting Information. ^bBold entries indicate instances in which the designated normalized cross-peak intensity in the standard NOESY data is > 3 times that measured in either the selective NOESY or HOBS NOESY data.

Figures

Figure 1

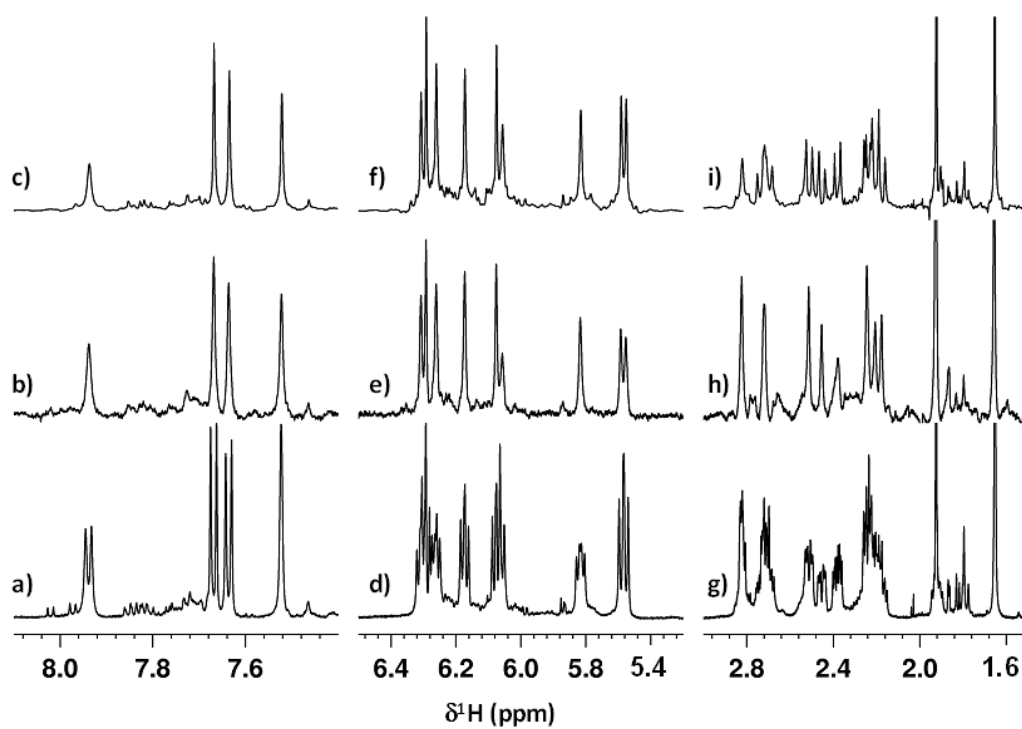


Figure 2

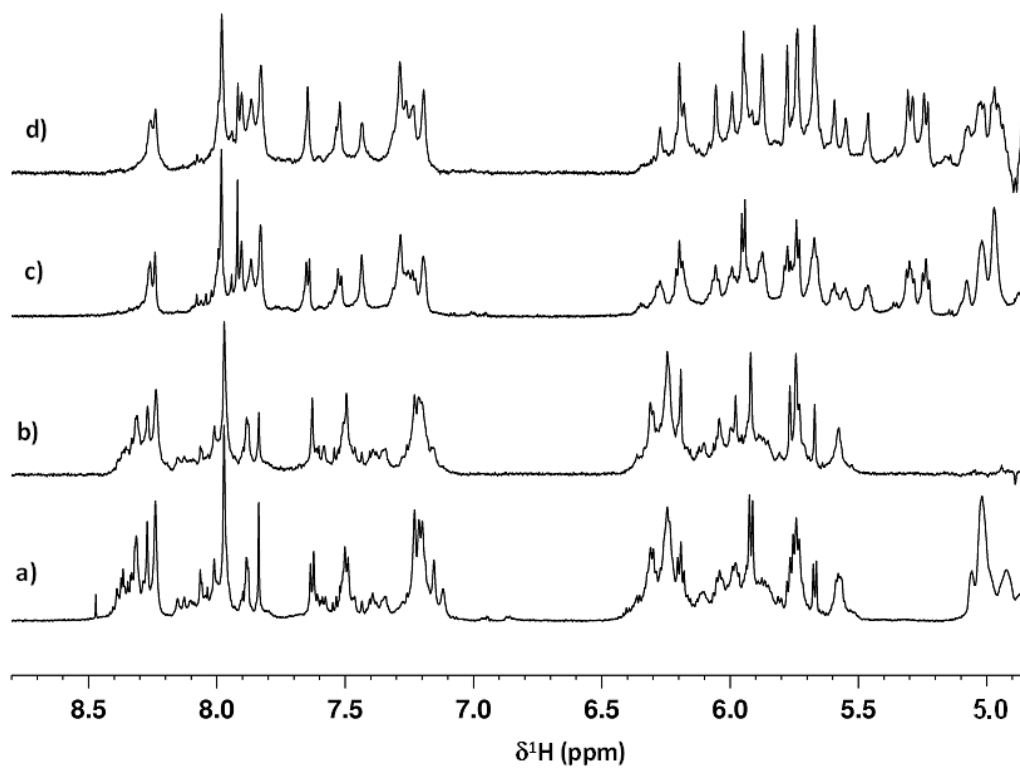


Figure 3

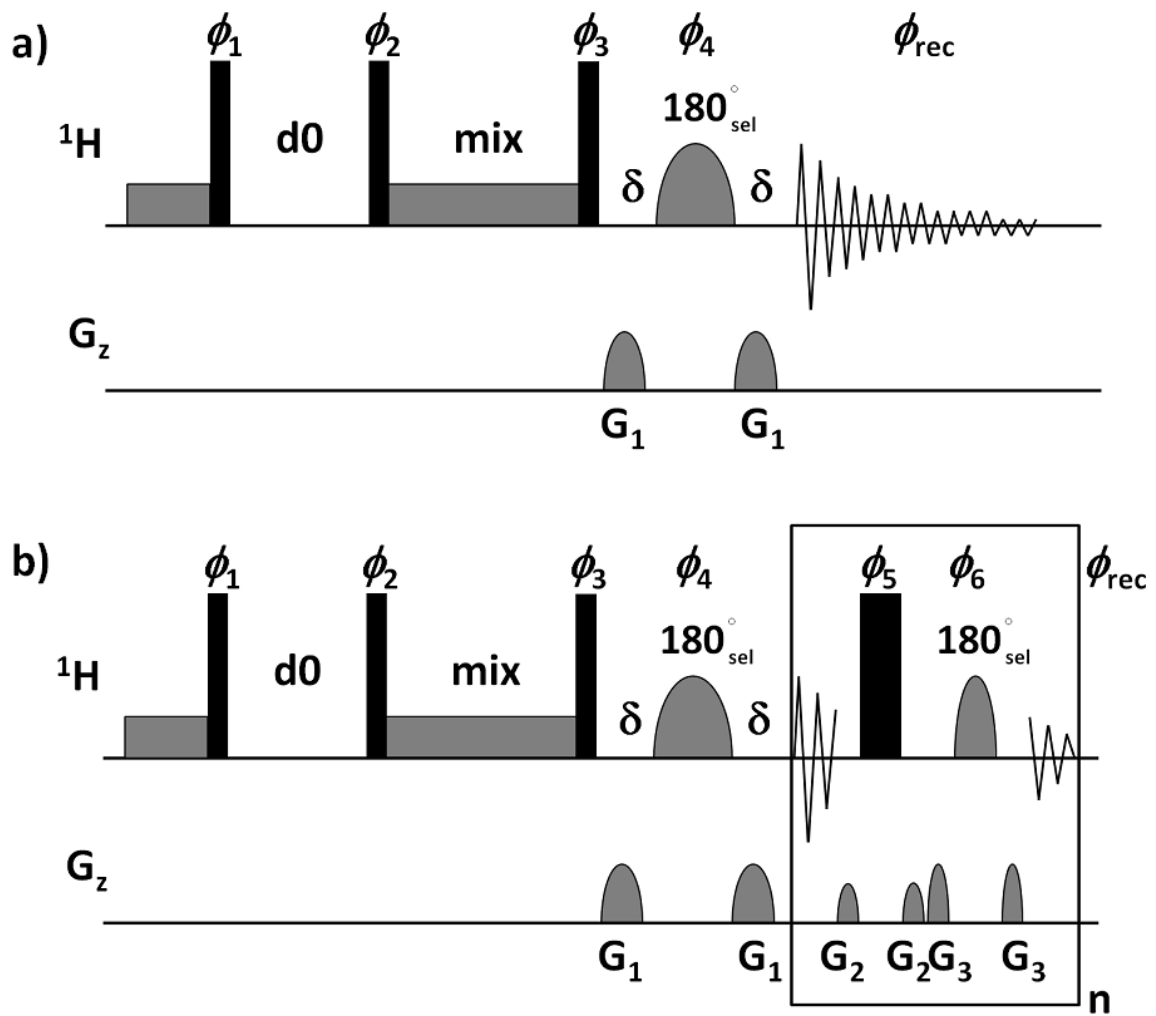


Figure 4

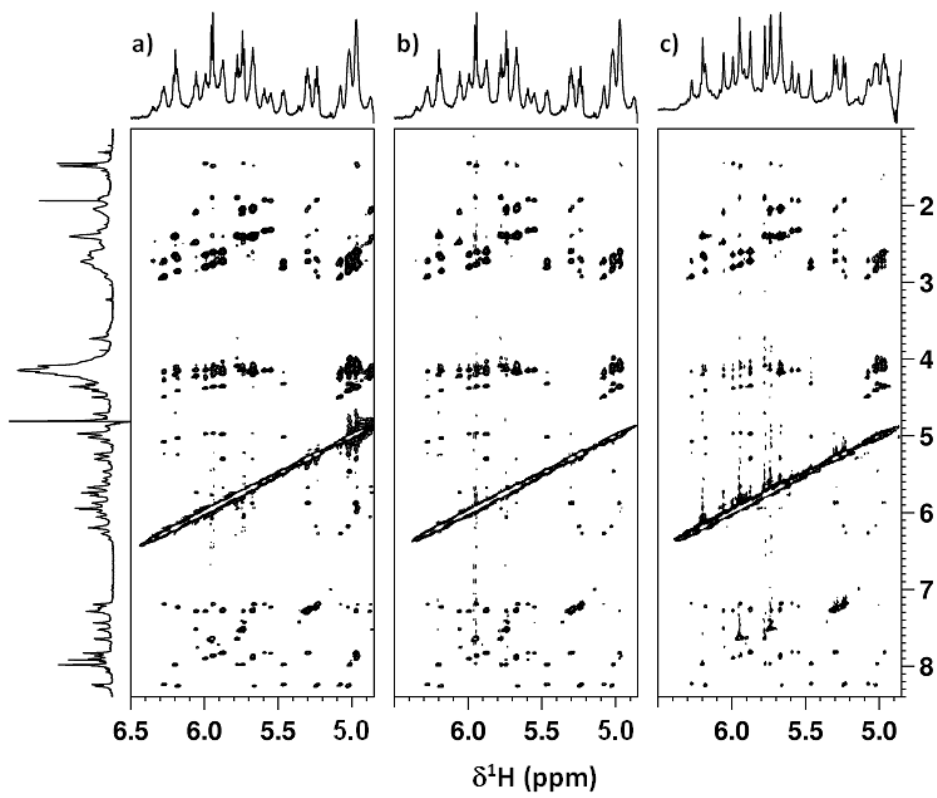


Figure 5

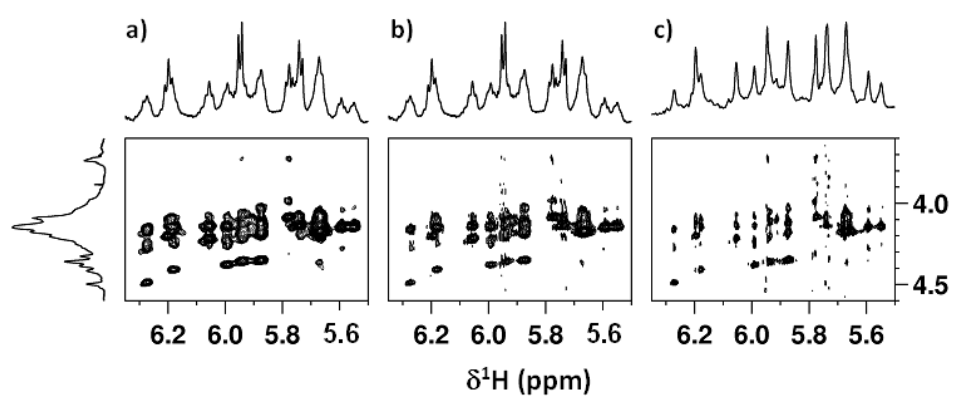


Figure 6

